THERMAL PROFILES AND FRACTION SOLID OF ALUMINIUM 7075 AT DIFFERENT COOLING RATE CONDITONS

A.H. Ahmad[1, 2, 3, a], S. Naher[1, 2] and D. Brabazon[1, 2]

[1]School of Mechanical and Manufacturing Engineering, Dublin City University, Dublin 9, Ireland

[2]Advanced Processing Technology Research Centre, Dublin City University, Dublin 9, Ireland

[3]Faculty of Mechanical Engineering, Universiti Malaysia Pahang, Pekan, Malaysia

[a]Email: asnul@ump.edu.my

Keywords: Thermal analysis, fraction solid, aluminium 7075, dendritic coherency point.

Abstracts: In order to determine suitable processing conditions for semi-solid aluminium 7075 thermal analysis (TA) was performed in order to obtain the relationship between fraction solid and temperature. During experimental work, the alloy was heated to 750°C by resistance heated box furnace and solidified at various cooling rates. Cooling curves for the metal were recorded with two thermocouples, one at the centre of the melt volume and one beside the containing crucible wall. A specially designed chamber with kaowool blanket was used to achieve the slowest cooling rate. The faster cooling rate was achieved with the crucible in open atmosphere with a set air flow rate over the crucible. A Data Acquisition (DAQ) system controlled by LabVIEW software was used to record the temperature-time profiles. From these cooling curves, the phase change at any corresponding time and temperature was estimated. The temperature difference between centre and wall of crucible was used to determine dendritic coherency point (DCP). Results show that, the slowest cooling rate with the kaowool blanket was at 0.03°C/s. An intermediate cooling rate of 0.21°C/s was achieved by leaving the melt to cool without kaowool blanket or forced air flow, and the fastest cooling rate was 0.43°C/s. The change in cooling rate altered the temperatures at which phase changes occurred, including those for eutectic and solidus. It was found that for lower the cooling rates that the DCP occurred at lower temperatures. The DCP for the cooling rate of 0.03°C/s was found to be 574°C (corresponding to 0.85 fraction solid) whereas the DCP for 0.43°C/s was found to be 623°C (corresponding to 0.55 fraction solid).

Introduction

Most aluminium semi-solid formed components are made from casting alloys such as A356 and A357 due to their fluidity. The cast series of aluminium alloys however have relatively poor mechanical properties compared to conventional wrought aluminium alloys. Wrought aluminium alloys have significant advantages in terms of higher ultimate tensile strength (UTS) and yield strength. Wrought aluminium 7075 is one of the aluminium alloys that has the highest tensile properties [1]. Components produced using this alloy includes aircraft fittings, gears and shafts, fuse parts, regulating valve parts, and worm gears [2]. STAMPAL-Italy [3], Grove Aircraft Landing Gear Systems Inc.-USA [4], ALCOA-USA [5] and JJ Churchill Ltd-UK [6] are among the list of companies who produce a wide range of the components using 7075.

Aluminium 7075 has recently been investigated for use in the of semi-solid metal (SSM) processing [7-12]. The performance of aluminium 7075 was investigated using both thixoformed cooling slope and recrystallization and partial melting (RAP) route in order to compare their mechanical properties [7]. It was noted in this work that the thixoformed RAP route produced better tensile properties.

A common problem that normally occurs during processing conventional extrusion of tubes is the formation of a welding line defect [9]. It was found from this work that the homogenous and equiaxed grain structure used for thixoextrusion of 7075 could be more easily shaped which resulted in elimination of the welding line defects and a lower energy requirement for processing compared with conventional extrusion processes.

Vaneetveld et al. found that superior mechanical properties resulted from the use of a higher tool temperature setting and appropriate tool punch speed during thixoforming [10]. These settings so adjusted resulted in reduced cracking which was noted to occur due to overly fast cooling rates. Aluminium 7075 has low sensitivity to temperature variation at high fraction solid which makes it more suitable for the high fraction solid thixoforging compared to other alloy systems [13].

Microstructure and elemental chemical measurement are two inspection methods that normally used to characterise and control melt quality of the alloy. Thermal analysis (TA) is another useful and important characterisation method which allows determination of the quality of a melt batch via recording of phase change temperatures and fraction solid-temperature profiles [14].

Differential thermal analysis (DTA) and differential scanning calorimetry (DSC) are among a list of thermal analysis methods. Both of these techniques use a sample to be tested and a reference sample. During testing, the change of temperature and energy between these two samples is plotted against time. DTA uses the concept of measuring changes of temperature in the sample, DSC however measures the energy difference between the samples directly [15]. Another thermal analysis technique uses two thermocouples to measure the heat change in a single sample. In this method the temperature difference between the solidification cooling curves at two separate points within the melt can be used to determine the dendritic coherency points (DCP) [16]. The DCP is where the point during solidification where the dendrites begin to impinge on one another across the solidifying system and where the metal strength begins to develop [16, 17]. The solidifying metal has negligible shear strength before DCP compared to after this coherency point occurs where the dendritic network has formed. This point is therefore accompanied by a significant increase system viscosity and strength [17].

In the solidification process, the heat loss may be equated to the heat conducted away and can be formulated according to equation (1) as follows:

$$V\ \rho\ C_p \left.\frac{dT}{dt}\right|_{bc} = V\ k(T_{metal} - T_{mould}) \tag{1}$$

where V is the volume, ρ is the density, C_p is the specific heat coefficient, $\left.\frac{dT}{dt}\right|_{bc}$ is rate of change of the base line curve, k is the thermal conductivity and $(T_{metal} - T_{mould})$ is the difference between the temperature of the metal and mould. The latent heat, H that evolves during solidification can be represented by equation (2) as follows:

$$\frac{dH}{dt} - V\ \rho\ C_p\ \left.\frac{dT}{dt}\right|_{bc} = V\ k(T_{metal} - T_{mould}) \tag{2}$$

Adding equation 1 and 2 gives a relation between the effects of latent heat on dT/dt curve that can be written as in equitation (3):

$$\frac{dH}{dt} = V\ \rho\ C_p \left[\left.\frac{dT}{dt}\right|_{cc} - \left.\frac{dT}{dt}\right|_{bc}\right] \tag{3}$$

The fraction solid f_s, present at a given time (t_1) during solidification is expressed by equation 4 where the ratio of the amount of latent heat evolution until time t_1, to the total amount of latent heat evolution during solidification can be written as:

$$f_s = \frac{\int_{t_0}^{t_1} dH}{\int_{t_0}^{t_f} dH} = \frac{\int_{t_0}^{t_1} \left[\left.\frac{dT}{dt}\right|_{cc} - \left.\frac{dT}{dt}\right|_{bc} \right] dt}{\int_{t_0}^{t_f} \left[\left.\frac{dT}{dt}\right|_{cc} - \left.\frac{dT}{dt}\right|_{bc} \right] dt} \quad (4)$$

There is interest in being able to process 7075 within the semi-solid state due to the enhanced properties available from this alloy compared especially to cast alloy alternatives. Wrought alloys are however more difficult to process within the semi-solid state due to their narrow solidification ranges and higher propensity for hot tearing. There is currently a lack of detailed experimental investigation within the literature into the thermal profiles for 7075 at various solidification rates which may occur during thixoforming. To understand the relationship between solidification rate, metallurgical behaviour, and fraction phase evolution, the experimental work presented below was conducted. In particular, the liquidus, eutectic and solidus temperature, fraction solid, dendritic coherency point effect resulting from the different cooling conditions have been determined.

Experimental Procedure

The chemical composition of the 7075 alloy used in this work, as determined with Oxford Instruments Inca X-act and micro-analysis EDXS and from the literature, is presented in Table 1.

Table 1: The chemical composition of the aluminium 7075

Source	(wt%) Al	Cr	Cu	Fe	Mg	Mn	Si	Ti	Zn
Experiment	88.5	0.20	2.02	0.24	2.38	0.12	0.14	0.09	6.04
Bäckerud [16]	Bal	0.19	1.36	0.28	2.49	-	0.11	-	-
ASM [2]	87.1-91.4	0.18-0.28	1.2-2.0	<0.5	2.1-2.9	<0.3	<0.4	<0.2	5.1-6.1

The graphite crucible used to melt the metal was of 100mm diameter and 100mm height. A billet weight of 1kg was placed in crucible before each experiment. The crucible was then heated to a temperature 750°C $\pm$5 by using resistance heated Carbolite 1600 box furnace. The crucible with molten metal was then transferred to the kaowool chamber in order to achieve the slow cooling rate, allowed to cool naturally without kaowool blanket for the intermediate cooling rate, or placed in a forced air flow to achieve the highest cooling rate. The specially designed chamber with kaowool insulation contained 100 mm of kaowool beneath the crucible, 50 mm side walls, and a 40 mm thick top layer of kaowool in order to ensure very slow cooling. Chromel-alumel K-type thermocouples were located at two different locations, one at the centre of the crucible and one at 35 mm from the centre closer to the crucible wall. Both thermocouples were immersed within the metal to a depth of 45 mm from the top of the melt. After the cooling curves were captured, the cooling rates were calculated from the portion of the cooling curve below the solidus temperature (between 50°C and 150°C below the solidus temperature).

The schematic of experimental set-up for slow cooling rate is shown in Fig. 1. The temperature versus time cooling curve data was recorded by using a NI 6036 data acquisition (DAQ) card with cold junction compensation. A series programs developed in LabVIEW allowed control of data acquisition rate, as well as calculation of the cooling curve differential (dT/dt curves) and fraction solid with respect to time. A DAQ rate of 500 Hz was set. For the slow cooling rate conditions this equated to 4,500,000 data points captured during the experiment period of two and a half hours. For the intermediate and fast cooling rate conditions there were approximately 800,000 data points (27 minutes) and 550,000 data points (18 minutes) respectively. A base line was constructed on the

dT/dt curves to represent the cooling rate which would have occurred in the absence latent heat evolution. The area between this curve and the actual cooling curve differential was calculated at each time point and divided by the total area between these curves in order to determine the fraction solid versus time curves, as per equation 4. Separately, the temperature recorded from the thermocouple at the crucible wall was subtracted from the temperature reading from the centre thermocouple at each time. This temperature difference was plotted against time. The DCP was then determined by identifying the maximum difference between these two readings.

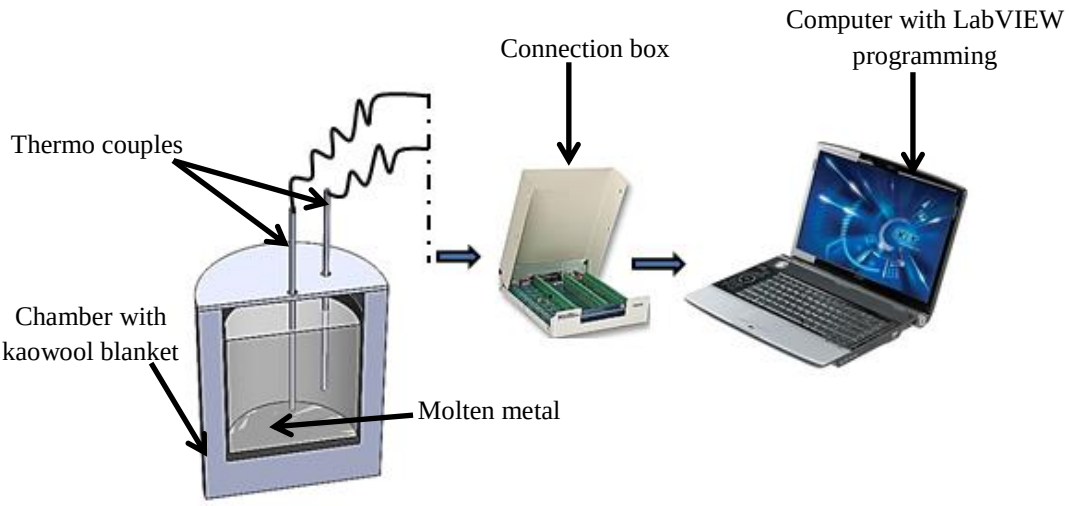

Figure 1: Schematic for thermal analysis experiment set-up for slow cooling rate by using two thermocouples method.

Results and Discussion

Thermal Analysis

The cooling curve for the slow cooling rate condition (at a cooling rate of 0.03°C/s) is shown in Fig. 2 (a). The liquidus, eutectic and solidus temperature were at 639.9°C, 470.2°C and 467.6°C respectively. The first derivation of the cooling curve with baseline is presented in Fig. 2 (b). This derivation curve allows identification of the phase changes that occurred in the alloy during the solidification period. The vertical lines in Fig. 2 (b) represent the start (liquidus) and end (solidus) of solidification. The calculated fraction solid versus temperature graph is shown in Fig. 2 (c). The information in Fig. 2 (c) is particularly useful for determining processing temperature settings for semi-solid metal processing.

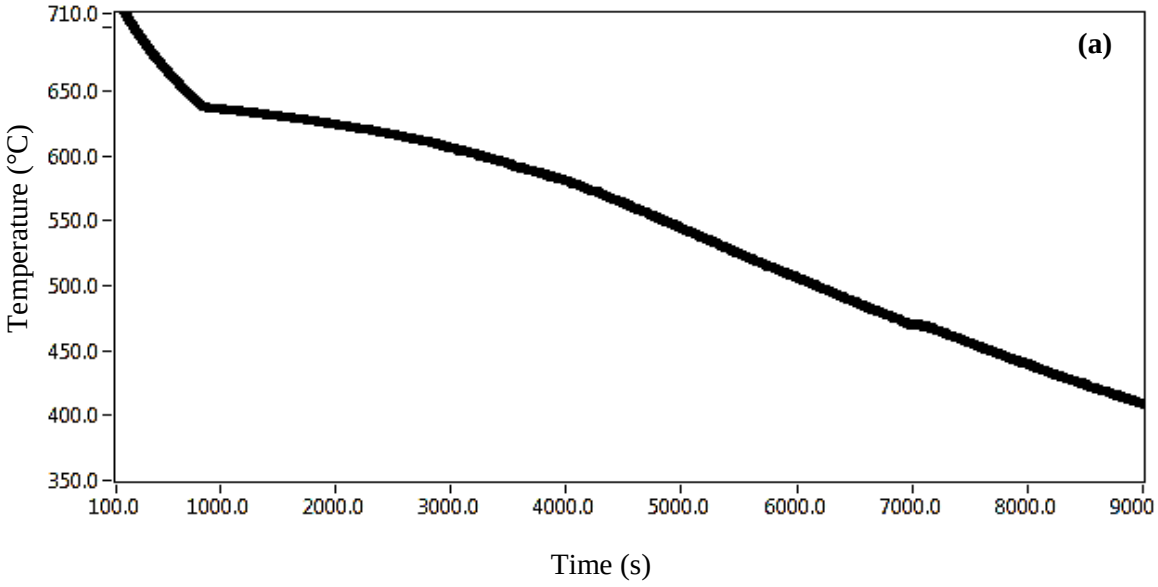
(a)
Temperature (°C)
710.0
650.0
600.0
550.0
500.0
450.0
400.0
350.0
100.0
1000.0
2000.0
3000.0
4000.0
5000.0
6000.0
7000.0
8000.0
9000
Time (s)

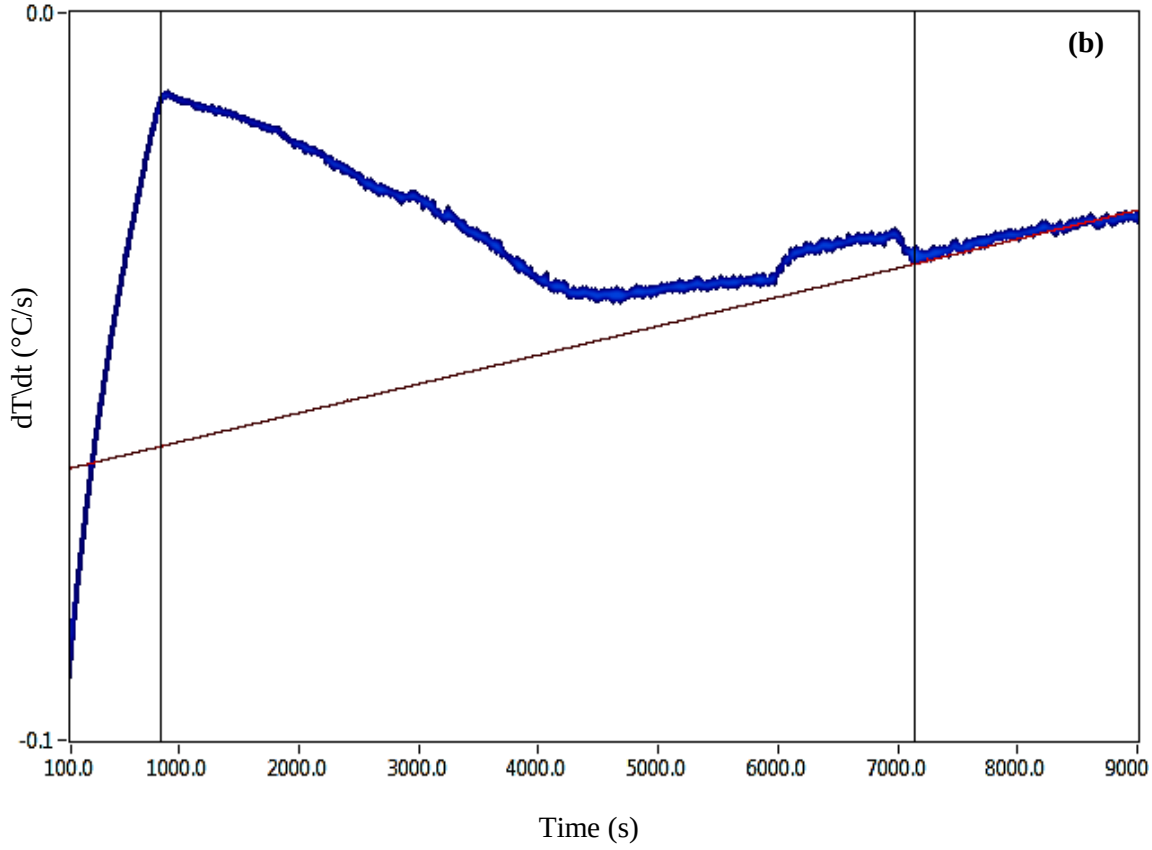
(b)
dT\dt (°C/s)
0.0
-0.1
100.0
1000.0
2000.0
3000.0
4000.0
5000.0
6000.0
7000.0
8000.0
9000
Time (s)

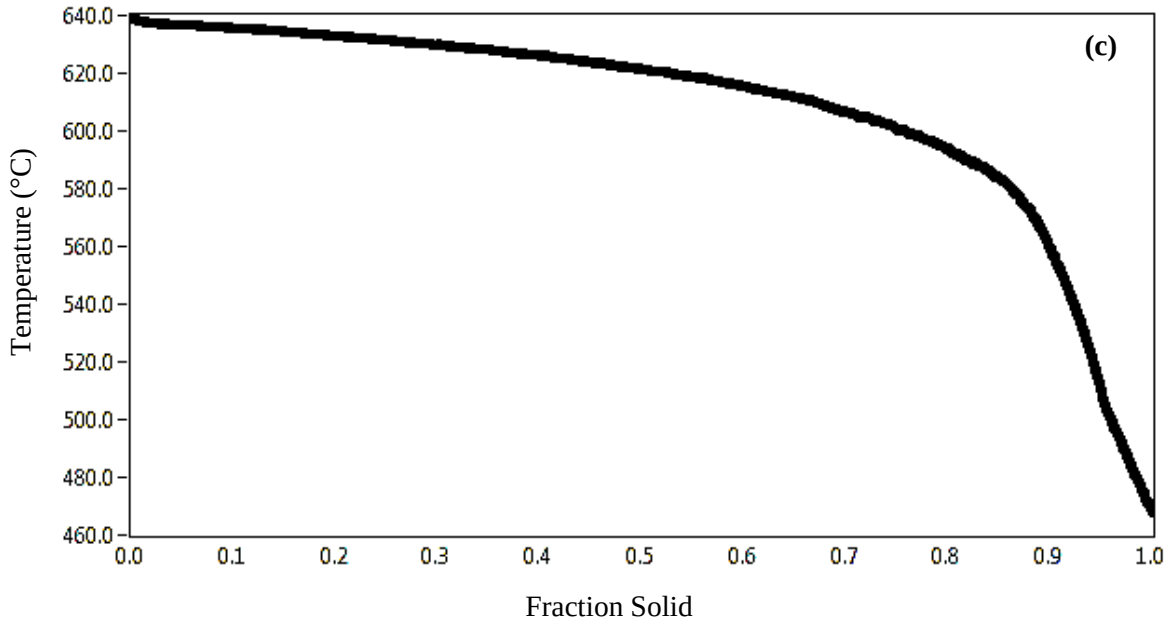

Figure 2: For cooling rate of 0.03°C/s the (a) cooling curve, (b) cooling curve derivate with respect to time (with baseline), and (c) calculated temperature-fraction solid relation.

The cooling curve for the intermediate cooling rate condition (at a cooling rate of 0.21°C/s) is shown in Fig. 3 (a). The liquidus, eutectic and solidus temperature were at 638.3°C, 474.7°C and 470.2°C respectively. Fig. 3 (b) shows the first derivation of the cooling curve with baseline as well as vertical lines indicating the start and end of the solidification. The corresponding calculated relationship between fraction solid and temperature presented in Fig. 3 (c).

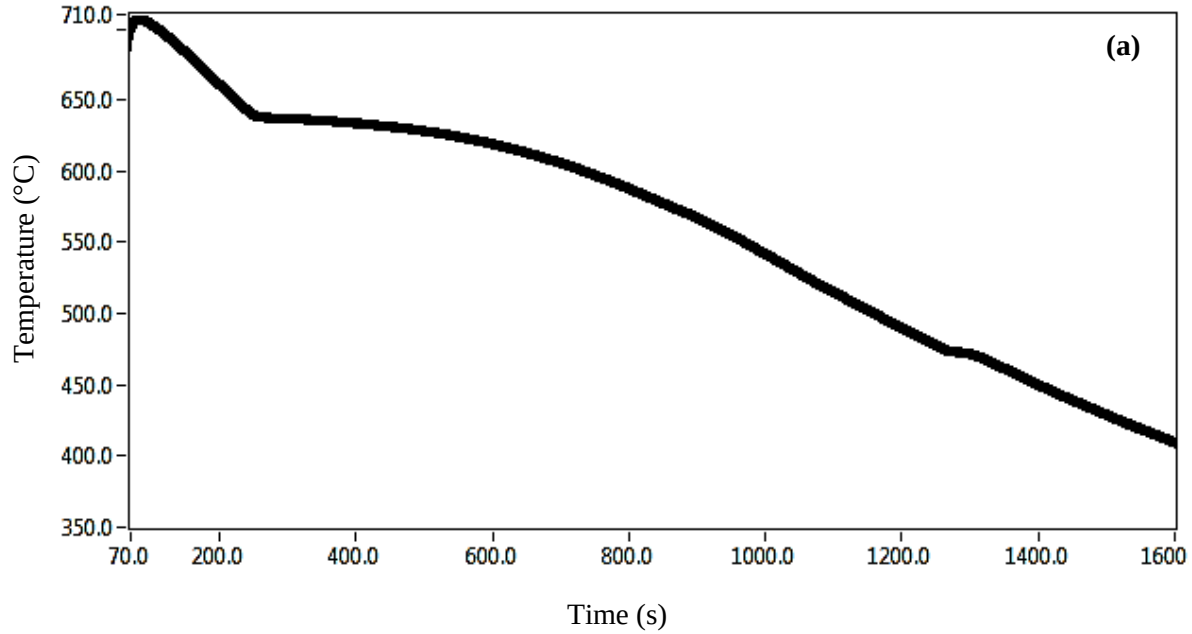

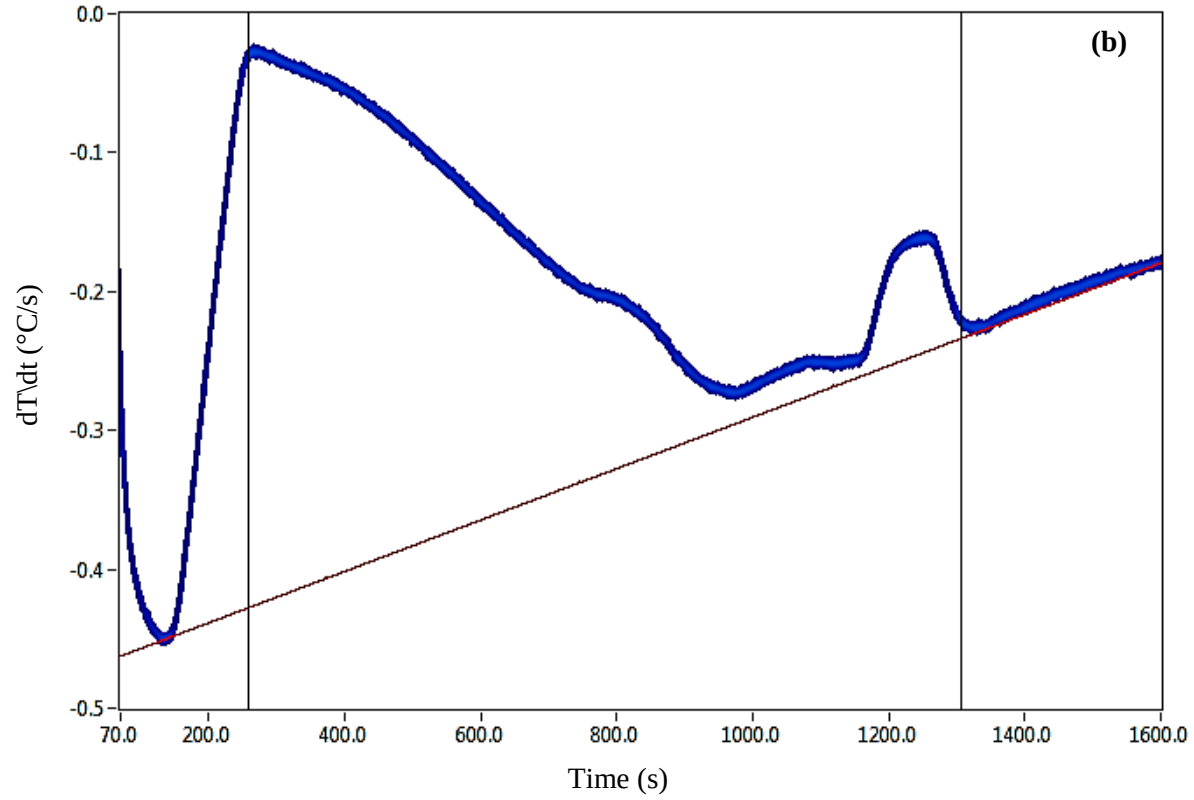

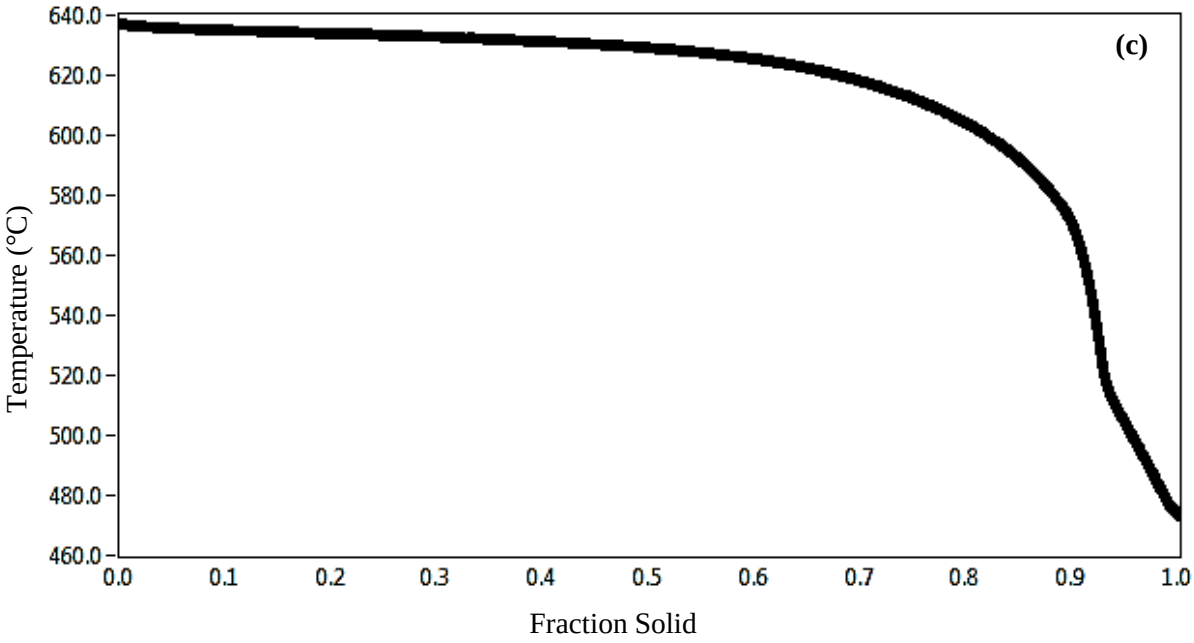

Figure 3: For cooling rate of 0.21°C/s the (a) cooling curve, (b) cooling curve derivate with respect to time (with baseline), and (c) calculated temperature-fraction solid relation.

The cooling curve for the intermediate cooling rate condition (at a cooling rate of 0.43°C/s) is shown in Fig. 4 (a). The liqudus, eutectic and solidus temperature were at 636.7°C, 477.2°C and 472.8°C respectively. Fig. 4 (b) shows the first derivation of the cooling curve with baseline as well as vertical lines indicating the start and end of the solidification. The corresponding calculated relationship between fraction solid and temperature presented in Fig. 4 (c).

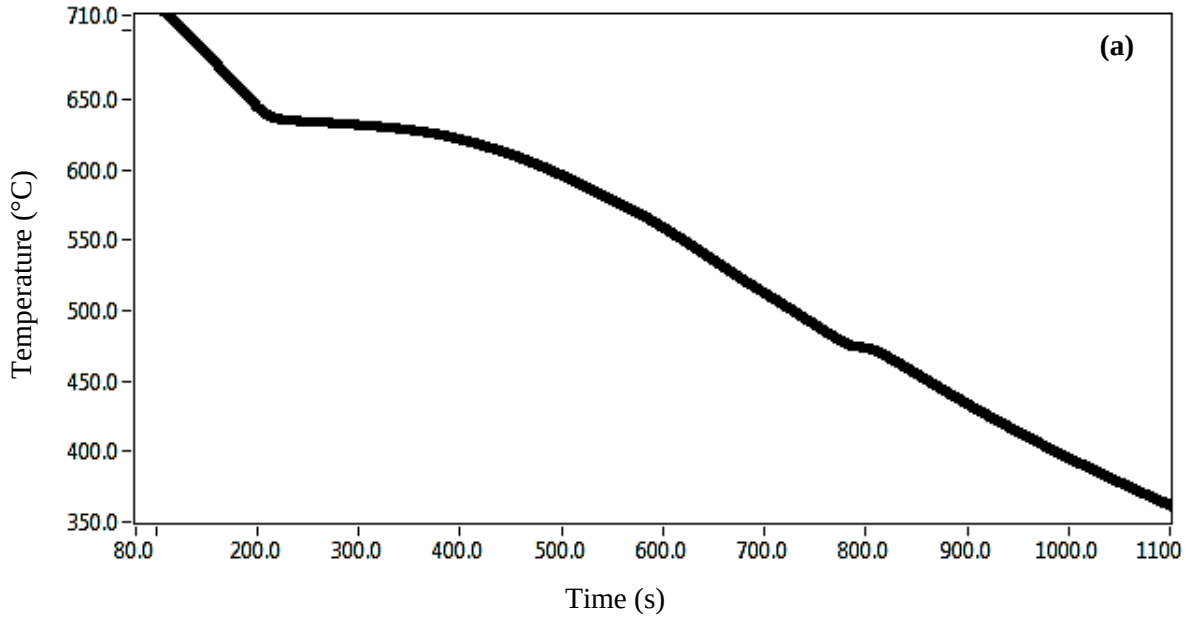
(a)
Temperature (°C)
710.0
650.0
600.0
550.0
500.0
450.0
400.0
350.0
80.0
200.0
300.0
400.0
500.0
600.0
700.0
800.0
900.0
1000.0
1100
Time (s)

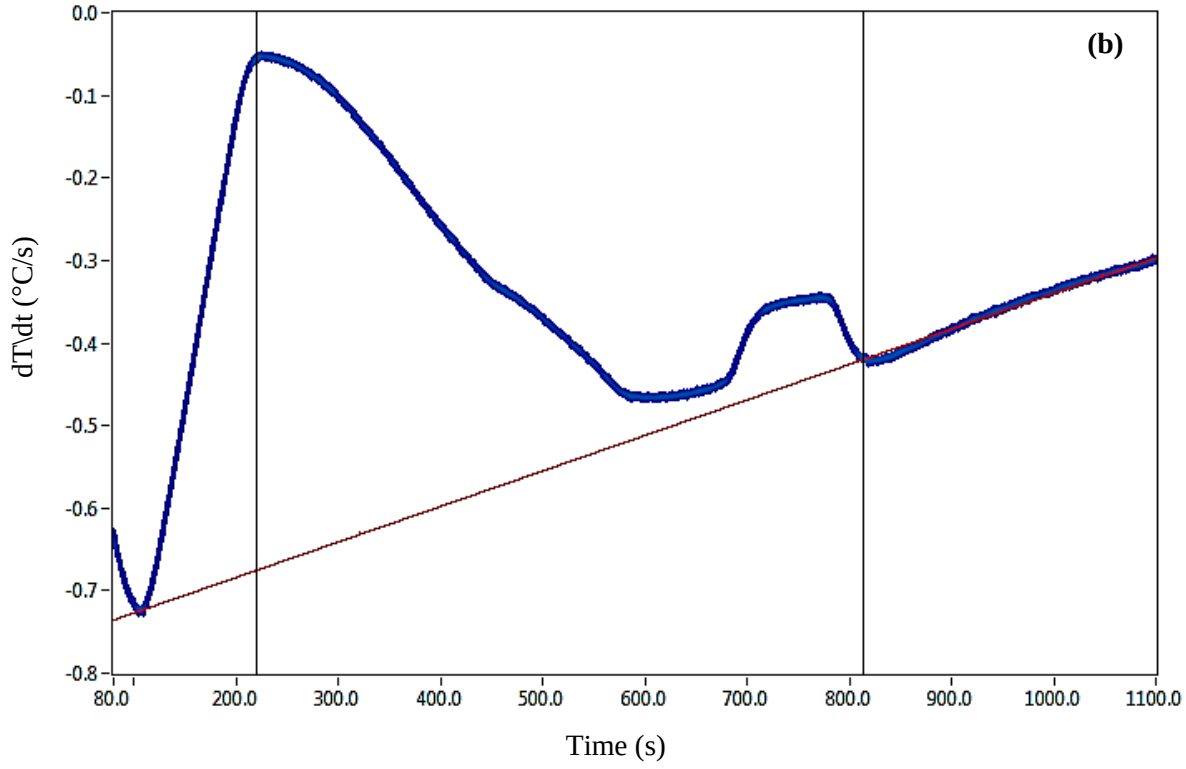
(b)
dT\dt (°C/s)
0.0
-0.1
-0.2
-0.3
-0.4
-0.5
-0.6
-0.7
-0.8
80.0
200.0
300.0
400.0
500.0
600.0
700.0
800.0
900.0
1000.0
1100.0
Time (s)

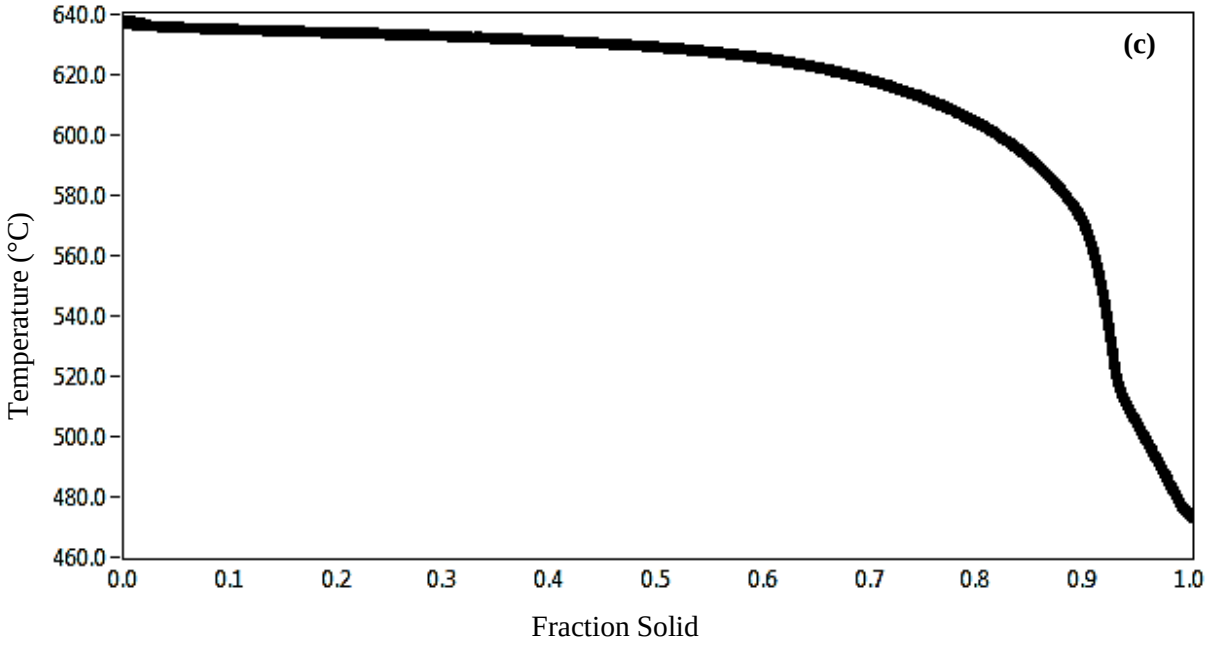

Figure 4: For cooling rate of 0.43°C/s the (a) cooling curve, (b) cooling curve derivate with respect to time (with baseline), and (c) calculated temperature-fraction solid relation.

Dendritic Coherency Points (DCP)

The two thermocouples method is designed specifically to measure the coherency point of the sample. The temperature differences between the first and second thermocouples are shown in Fig. 5 (a), (b), and (c) for the slow, medium and high cooling rates respectively. The time at which coherency occurs and hence corresponding temperature and fraction solid can be determined by the occurrence of the maximum difference between these two thermocouples. The coherency point for a cooling rate of 0.03°C/s occurred at 4192.5s as shown in Fig. 5 (a). This value was then compared with the cooling curve in Fig. 2 (a) and which indicated that the coherency point was at 574.1°C. The coherency point for cooling rate of 0.23°C/s was at 513.4s and temperature of 627.3°C, see Fig. 5 (b) and Fig. 3 (a). Finally, the coherecy point for the cooling rate of 0.43°C/s was at 391.6s and temperature of 623.5°C, see in Fig. 5 (c) and Fig. 4 (a).

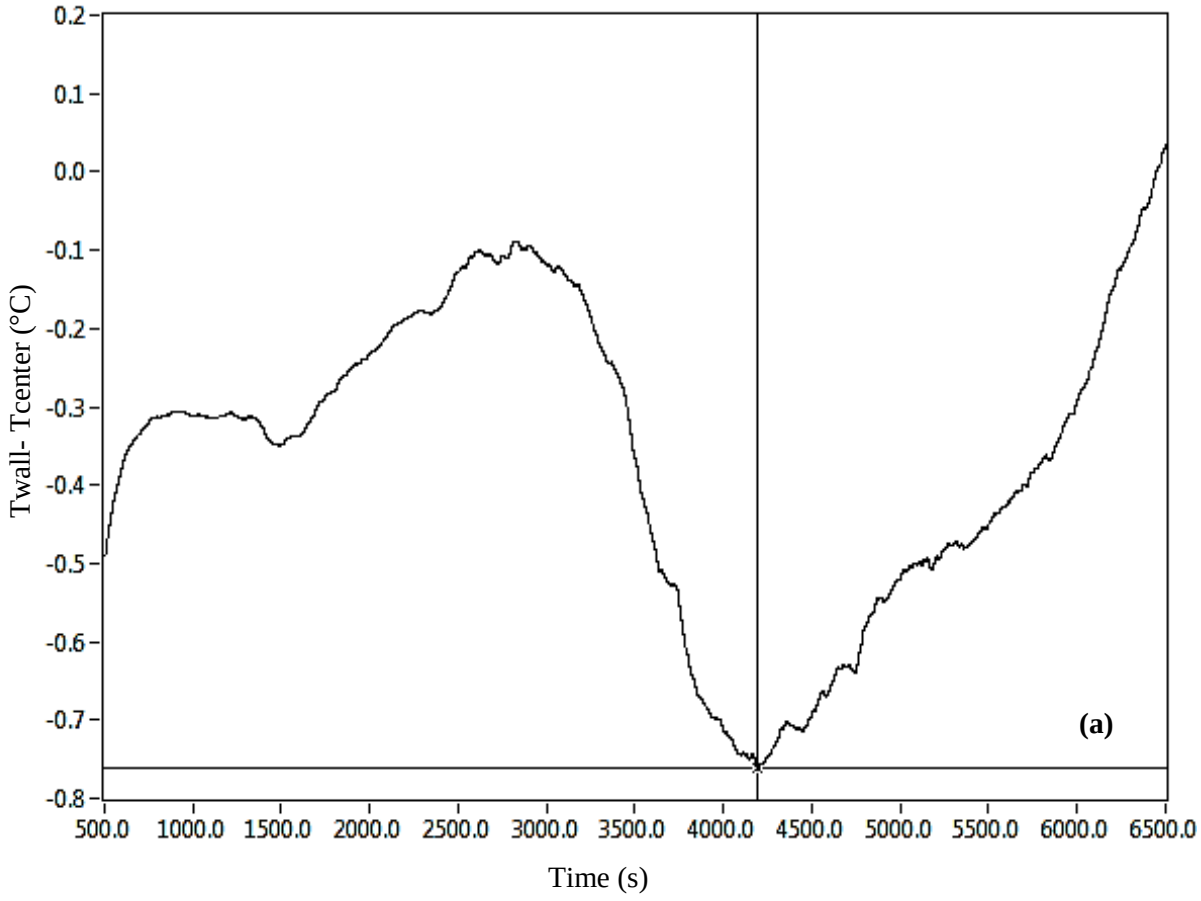
0.2
0.1
0.0
-0.1
-0.2
-0.3
-0.4
-0.5
-0.6
-0.7
-0.8
Twall- Tcenter (°C)
500.0
1000.0
1500.0
2000.0
2500.0
3000.0
3500.0
4000.0
4500.0
5000.0
5500.0
6000.0
6500.0
Time (s)
(a)

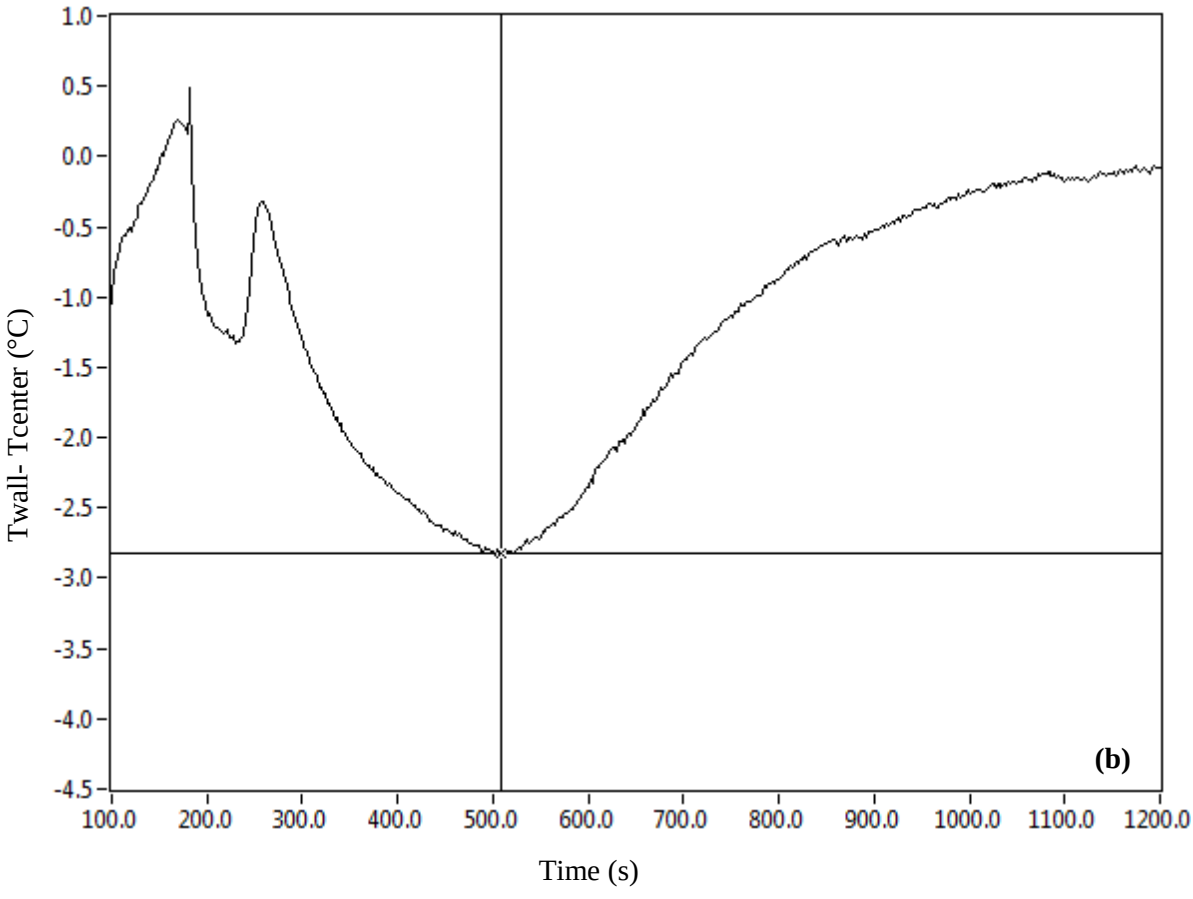
1.0
0.5
0.0
-0.5
-1.0
-1.5
-2.0
-2.5
-3.0
-3.5
-4.0
-4.5
Twall- Tcenter (°C)
100.0
200.0
300.0
400.0
500.0
600.0
700.0
800.0
900.0
1000.0
1100.0
1200.0
Time (s)
(b)

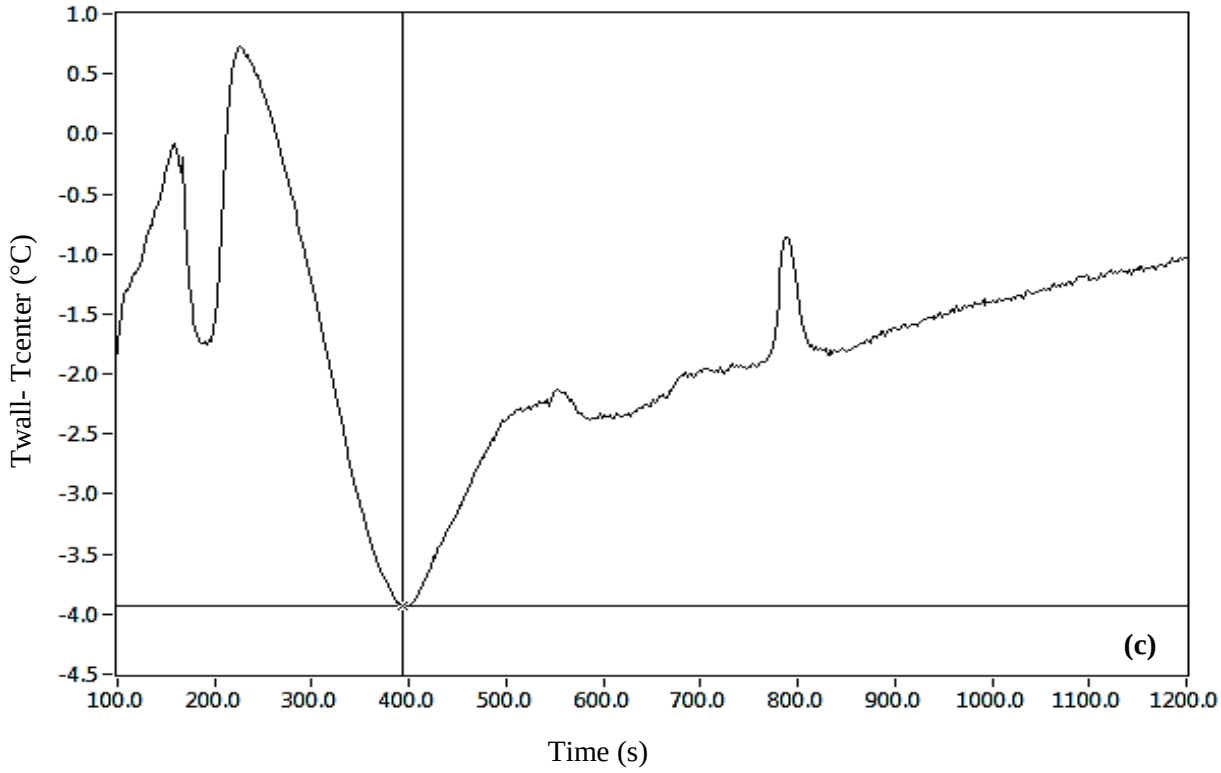

Figure 5: Temperature differences between thermocouples located at center and wall of the crucible with different cooling rates of (a) 0.03°C/s, (b) 0.21°C/s and (c) 0.43°C/s.

Effect of Cooling Rate on Solidification

The liquidus, eutectic, and solidus temperatures for various cooling rates from this work and from other reports are shown in Table 2. The experimental results from this work indicated no significant variation in the liquidus temperature for the different cooling rate conditions. The liquidus temperature found was slightly higher than other reported experimental results [2, 16]. This is commonly observed though due to variations in chemical composition of the alloy as received from different suppliers or at different times from the same supplier. The variation in alloying elements affect the overall solidification process and results in differences in temperature at which phase changes occur [20]. The different cooling rates resulted in altered solidification characteristic for 7075. The eutectic and solidus temperatures were noted to increase with the increasing cooling rate. These differences can been seen clearly between the eutectic and solidus temperatures for the cooling rates of 0.03°C/s and 0.43°C/s.

Table 2: Liquidus, eutectic and solidus temperature at different cooling rates.

Source	Cooling Rate (°C/s)	Liquidus Temp.(°C)	Eutectic Temp.(°C)	Solidus Temp.(°C)
This work	0.03	639.9	470.2	467.6
This work	0.21	638.0	474.7	470.2
This work	0.43	638.2	477.2	472.8
Bäckerud [16]	0.30	630.0	469.0	469.0
Bäckerud [16]	0.70	630.0	470.0	470.0
ASM [2]	-	635.0	-	477.0

Effect of Cooling Rate on Dendrite Coherency Point (DCP)

Table 3 shows the temperatures at which coherency occurred for the different cooling rates from the work of Bäckerud et al. and this work. For the results measured in this work, it was found that the DCP temperature increased from 574°C to 627°C for a cooling rate increase from 0.03°C/s to 0.21°C/s. A further increase in cooling rate to 0.43°C/s was not found to change the coherency temperature significantly from that at 0.21°C/s. The fractions solids calculated at the coherency points were 0.85, 0.55 and 0.60 respectively for the cooling rates of 0.03°C/s, 0.21°C/s and 0.43°C/s. In SSM processing, knowledge of the coherency point is important. The shear strength of the semi-solid material increases greatly after this point. Knowledge of this point therefore allows a better understanding of material behaviour and determination of a suitable temperature for processing. Optimum fraction solids for thixoforging have been noted to be within the range of 0.3 to 0.5 [22, 23]. Delaying DCP to a lower temperature and higher fraction solid, by utilisation of a lower cooling rate, has the advantage of extending the temperature and fraction solid range over which the semi-solid material can be processed [17].

Table 3: Measured Dendritic Coherency Point (DCP) temperatures at different cooling rates.

Source	Cooling Rate (°C/s)	DCP Temperature (°C)
This work	0.03	574.1
This work	0.21	627.3
This work	0.43	623.5
Bäckerud [16]	0.30	623.0

Conclusion

In order to gain useful information of phase transformation temperatures from thermal analysis experimental work, a steady heat flow rate from the metal to the surrounding environment must be achieved to avoid cooling curve distortions which are not related to latent energy release effects [21]. This was achieved in this work with a specially designed insulated chamber to achieve the lowest cooling rate, cooling of the melt within the crucible in a quiescent open atmosphere for the medium cooling rate, and with use of a set air flow rate over the crucible to achieve the highest cooling rate. Cooling rate and fraction solid are important parameters for thixoforming. The thermal analysis performed on the captured experimental cooling curves within this work has shown that the different cooling rates have had a significant effect to the liquidus, eutectic and solidus phase change temperatures. The temperatures for specific fraction solids and coherency points were also found to be strongly dependent on cooling rate. Below the coherency points, the slopes of the fraction solid curves were not very steep which indicates that the fraction solid is not overly sensitive to temperature fluctuation within this region. These results are very encouraging that suitable processing conditions can be applied for the thixoforming of 7075.

Acknowledgement

The authors would also like to acknowledge the support from Dublin City University and the Ministry of Higher Education, Malaysia for funding this work.

References

[1] Kaufman JG. *Introduction to aluminium alloys and tempers.* ASM International: United State of America, **2000**.

[2] *Metals Handbook, Vol.2 - Properties and Selection: Nonferrous Alloys and Special-Purpose Materials.* ASM International: **1990**.

[3] STAMPAL. *http://www.stampal-sb.si/* [Accessed 25 Nov 2012].

[4] GROVE AIRCRAFT. *http://www.groveaircraft.com/* [Accessed 25 Nov 2012].

[5] ALCOA. *http://www.alcoa.com/global/en/home.asp* [Accessed 25 Nov 2012].

[6] JJ CHURCHILL LTD. *http://jjchurchill.com/* [Accessed 25 Nov 2012].

[7] Liu D, Atkinson HV, Kapranos P, Jirattiticharoean W, Jones H. *Microstructural evolution and tensile mechanical properties of thixoformed high performance aluminium alloys.* Materials Science and Engieering A **2003**, *A361*, 213-224.

[8] Chayong S, Atkinson HV, Kapranos P. *Thixoforming 7075 aluminium alloys.* Materials Science and Engineering A **2005**, *A390*, 3-12.

[9] Don-In Jang, Young-Ok Yoon, Shae K Kim. *Thixoextrusion for 7075 Aluminium wrought alloy tube.* Semi-Solid Processing of Alloys and Composites X **2008**, *141-143*, 267-270.

[10] Vaneetveld G, Rassili A, Pierret JC, Lecomte-Beckers J. *Improvement in thixoforging of 7075 aluminium alloys at high solid fraction.* Semi-Solid Processing of Alloys and Composites X **2008**, *141-143*, 707-712.

[11] Atkinson HV, Burke K, Vaneetveld G. *Recrystallisation in the semi-solid state in 7075 aluminium alloy.* Materials Science and Engineering A **2008**, *A490*, 266-276.

[12] Neag A, Favier V, Pop M, Becker E, Bigot R. *Effect of experimental conditions on 7075 aluminium response during thixoextrusion.* Key Engineering Materials **2012**, *504-506*, 345-350.

[13] Vaneetveld G, Rassili A, Pierret JC, Lecomte-Beckers J. *Conception of tooling adapted to thixoforging of high solid fraction hot-crack-sensitive aluminium alloys.* Transactions of Nonferrous Metals Society of China **2010**, *20*, 1712-1718.

[14] Emadi D, Whiting LV, Nafisi S, Gomashchi R. *Applications of thermal analysis in quality control of solidifications processes.* Journal of Thermal Analysis and Calorimetry **2005**, *81*, 235-242.

[15] Daniels T. *Thermal Analysis.* Kagon Page Limited: United Kingdom, **1973**.

[16] Bäckerud L, Chai G, Tamminen J. *Solidification Characteristics of Aluminium Alloys; Volume 2: Foundry Alloys.* University of Stockholm, **1991**.

[17] Dahkle AK SD. *Rheological behaviour of the mushy zone and its effects on the formation of casting defects during solidification.* Acta Metallurgica **1998**, *47*, 31-41.

[18] Farahany S, Bakhsheshi-Rad HR, Idris MH, Abdul Kadir MR, Lotfabadi AF, Ourdjini A. *In-situ thermal analysis and macroscopical characterization of Mg–xCa and Mg–0.5Ca–xZn alloy systems.* Thermochimica Acta **2012**, *527*, 180-189.

[19] Veldman N, Dahle AK, StJohn D, Arnberg L. *Dendrite coherency of Al-Si-Cu alloys.* Metallurgical and Materials Transactions A **2001**, *32*, 147-155.

[20] Arnberg L, Chai G, Backerud L. *Determination of dendritic coherency in solidifying melts by rheological measurements.* Materials Science and Engineering A **1993**, *173*, 101-103.

[21] Amin KM and Mufti Nadeem A. *Investigating cooling curve profile and microstructure of a squeeze cast Al–4%Cu alloy.* J. Mater. Process. Technol. **2012**, *212*, 1631-1639.

[22] Camacho AM, Atkinson HV, Kapranos P, Argent BB. *Thermodynamic predictions of wrought alloy compositions amenable to semi-solid processing.* Acta Metallurgica **2003**, *51*, 2319-2330.

[23] Haga T and Kapranos P. *Simple rheocasting processes.* Journal of Materials Processing Technology **2002**, *130-131*, 594-598.